

## Effects of Bath Temperature on Electrodeposited Permanent Magnetic Co-Pt-W(P) Films

Hongliang Ge,\* Qiong Wu, Guoying Wei, Xinyan Wang, and Qiaoying Zhou

College of Materials Science & Engineering, China Jiliang University, Hangzhou 310018, PR China

\*E-mail: hongliang\_ge@cjl.u.edu.cn

Received February 26, 2007

The effects of bath temperature on electrochemical behavior, alloy composition, crystallographic structure, morphology and the magnetic properties of electrodeposited Co-Pt-W(P) films were investigated. Electrochemical studies show that alloy electrodeposition has been shifted to more positive potentials and the critical time for nucleation decreased as electrolyte temperature increased. As the temperature increased from 40 °C to 80 °C, tungsten content in the deposit increased, while phosphorus content decreased. The films deposited at T = 40 °C exhibited soft magnetic properties. However, electrodeposited at T = 70 °C, the films exhibited hard magnetic properties. It is also demonstrated that higher temperature more than 70 °C could weaken hard magnetic properties. XRD results indicated that the deposits obtained at 50 °C-70 °C showed enhancement of [00.1] P.O. (preferred orientation) with the bath temperature, which resulted in the stronger perpendicular magnetic anisotropy.

**Key Words :** Co-Pt-W(P) thin films, Electrochemical deposition, Bath temperature

### Introduction

Numerous studies have been carried out to develop Co-based hard magnetic thin films because of potential application in electromagnetic-actuated microelectromechanical systems (MEMS).<sup>1-3</sup> Co-Pt films are of particular interest in this respect as they can provide large magnetocrystalline anisotropy, coercivity, and high resistance to oxidation and corrosion.<sup>4-6</sup> These alloy films can be grown by electro-deposition process, which has many advantages over vacuum process: low cost, easy maintenance, and the ability to "tailor" deposit shape, structure and property.<sup>7</sup>

The electrodeposition of Co-Pt-W(P) alloys, with reduced Pt content and improved magnetic properties at high deposit thickness has been studied in recent years.<sup>8</sup> The magnetic properties of electrodeposited alloys can be related to their composition and crystallographic structure, which depend on the electrochemical parameters, including the electrolyte composition, current density, bath pH and temperature.<sup>9</sup> In P. L. Cavallotti's work,<sup>7</sup> the effect of temperature on Co-Pt-Zn(P) layers was considered. By increasing temperature from 50 to 80 °C, cobalt content slightly increased, while zinc and platinum contents were almost constant. Deposit faradaic efficiency was not much influenced by temperature.<sup>10</sup> By far, there were no publications about the effect of bath temperature on Co-Pt-W(P) electrodeposition.

In our paper, chronopotential analysis and cyclic voltammetry investigation have been utilized to study the nucleation and growth mechanism of Co-Pt-W(P) electrodeposition, and the effects of electrodeposition temperature on film composition, crystallographic structure, morphology and magnetic properties are discussed.

**Table 1.** Bath composition of Co-Pt-W(P) electrodeposit

Chemical	Concentration (mol/L)
CoSO <sub>4</sub> ·7H <sub>2</sub> O	0.1
(NH <sub>4</sub> ) <sub>2</sub> PtCl <sub>6</sub>	0.01
Na <sub>2</sub> WO <sub>4</sub> ·2H <sub>2</sub> O	0.27
(NH <sub>4</sub> ) <sub>2</sub> C <sub>6</sub> H <sub>6</sub> O <sub>7</sub>	0.2
NaH <sub>2</sub> PO <sub>4</sub> ·2H <sub>2</sub> O	0.05

### Experimental Details

The plating solutions were prepared from analytical grade chemicals and distilled water. Solution compositions (unless otherwise noted) were optimized in our former work,<sup>11</sup> listed in Table 1. (NH<sub>4</sub>)<sub>2</sub>C<sub>6</sub>H<sub>6</sub>O<sub>7</sub> was added as complexing agent.

Co-Pt-W(P) films were electrodeposited in a classical three-electrode glass cell. The substrates were copper sheets. Before experiment, substrates were polished with silicon carbide, and cleaned ultrasonically in acetone for 15 minutes. Then the substrate were activated by means of a dilute solution of sulphate acid and finally they were thoroughly rinsed with doubly distilled water. A platinum sheet was used as a counter electrode, and the reference electrode was a saturated calomel electrode (SCE). Electrolyte temperature was in the range of 40-80 °C, kept constant during electrodeposition. Current was supplied to the cell by means of a power supply in constant current mode. The current density was 12 mA·cm<sup>-2</sup>. The electrolyte pH was adjusted to 8.0 with either sodium hydroxide or sulphamic acid. The bath temperature was controlled to be constant by a thermostat during the experiment.

The chemical composition of thin films was measured by

energy dispersive spectrometer (EDS) (JED-2001, JEOL). Hysteresis loops were determined by vibrating sample magnetometer (VSM) (LakeShore 7407) in magnetic field both perpendicular and parallel to the substrate. The phase structure and texture of deposited films were determined by X-ray diffractometry (XRD) (X'Pert MPD Philips PW 1830). Atomic force microscopy (AFM) (DI 3000) was used to examine the morphology of the films.

## Results and Discussion

**Influence of temperature on the electrochemical behaviors.** In order to determine the electrochemical details of Co-Pt-W(P) electrodeposition, we investigated the solutions by means of cyclic voltammetry containing  $\text{CoSO}_4$ ,  $\text{Na}_2\text{WO}_4$ ,  $(\text{NH}_4)_2\text{PtCl}_4$  and  $(\text{NH}_4)_2\text{C}_6\text{H}_6\text{O}_7$ . Figure 1 shows that a sharp current increase attributed to Co-Pt-W(P) deposition and hydrogen evolution appeared in the negative scan. Meanwhile, during the inverse potential scan, it is possible to note a crossover of the cathodic and anodic branches, typical of the formation of a new phase, codeposition of Co-Pt-W(P), involving nucleation processes at 60 °C.<sup>12</sup> During the positive scan, a single oxidation peak was observed around -450 mV.

Nucleation was involved in every solution at different temperatures, see Figure 2. The comparison of the voltammograms, recorded from the solutions at different temperatures, revealed that alloy electrodeposition has been shifted to more positive potentials as the temperature increased: The codeposition of Co-Pt-W(P) began at -0.71 V when deposition temperature was kept at 40 °C; electrodeposition potential was -0.64 V at 60 °C and -0.62 V at 70 °C. This result suggests that the overpotential needed to start the electrodeposition process of alloy is less at higher temperatures, which was in accordance with the Nernst Equation. It was also noted that the Co-Pt-W(P) oxidation peak moved to more negative potentials when the bath temperature was

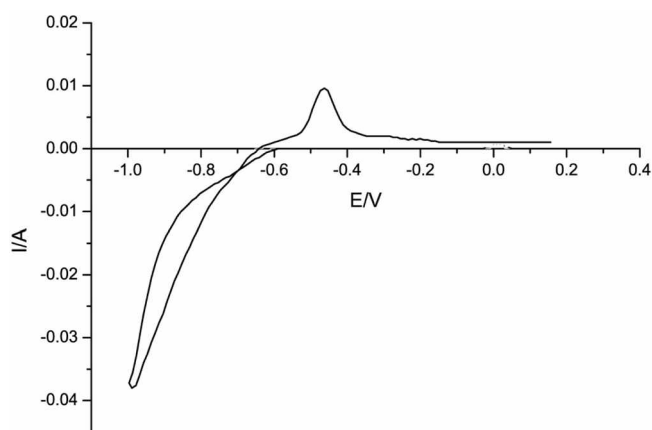


**Figure 1.** Typical CV curve obtained at the GC electrode in 0.1 mol/L  $\text{CoSO}_4$ , 0.27 mol/L  $\text{Na}_2\text{WO}_4$ , 0.2 mol/L  $(\text{NH}_4)_2\text{PtCl}_4$  and 0.2 mol/L  $(\text{NH}_4)_2\text{C}_6\text{H}_6\text{O}_7$  (pH = 8.0). T = 60 °C. The potential scan started at 0.1 V toward the negative direction and then reversed at -1.15 V, at a rate of 5 mV/s. Experiments were made under stirring condition.

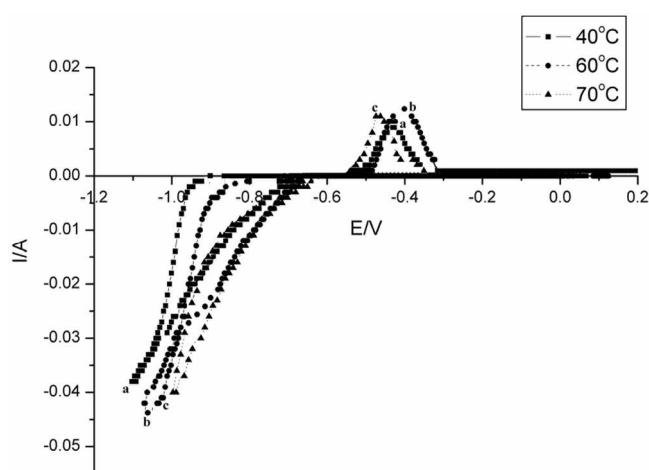


**Figure 2.** CV curves obtained at the GC electrode in  $\text{CoSO}_4$  0.1 M,  $\text{Na}_2\text{WO}_4$  0.27 M,  $(\text{NH}_4)_2\text{PtCl}_4$  0.2 M and citrate 0.2 M (pH = 8.5) system at different temperatures: (a) 40 °C, (b) 60 °C and (c) 70 °C. The potential scan started at 0.1 V toward the negative direction and then reversed at -1.15 V, at a rate of 5 mV/s. Experiments were made under stirring condition.

rising to 70 °C (Fig. 2, curve c), which implied that electrodeposited Co-Pt-W(P) thin films in the bath with the temperature of 70 °C were unstable compared to alloys electrodeposited from other temperatures. This is perhaps as a result of decrease of phosphor content in thin films (Figure 5).

Chronopotential analysis is a useful way to study the nucleation and growth mechanism of alloy electrodeposition. Galvanostatic typical potential-transient curves are shown in Figure 3 at different temperatures (current density is  $12 \text{ mA}\cdot\text{cm}^{-2}$ ). Each transient has one potential maximum followed by a sharp fall and subsequent growth, indicating nucleation behavior. It can be seen in Figure 3 that the critical time for nucleation decreased with temperature, which can lead to the increase of the nucleation number during the fixed time in accordance with the electrochemical nucleation formula.<sup>13</sup>

The influence of bath temperature on the Co-Pt-W(P) codeposition can be estimated by measuring changes in the efficiency, which was given by:  $100 \times m_{\text{exp}}/m_{\text{theo}}$  ( $m_{\text{exp}}$ :

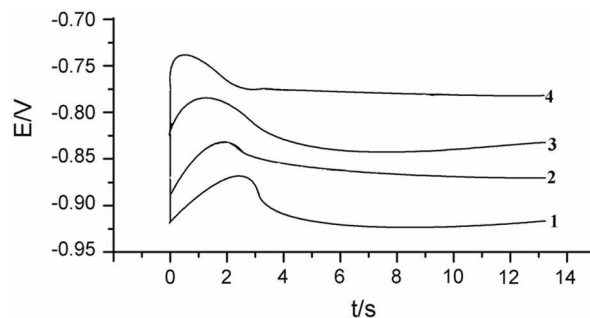


**Figure 3.** Galvanostatic E-t transients: 1. T = 40 °C 2. T = 60 °C 3. T = 70 °C 4. T = 80 °C (c.d. =  $12 \text{ mA}\cdot\text{cm}^{-2}$ ). Solution composition: 0.1 mol/L  $\text{CoSO}_4$ , 0.27 mol/L  $\text{Na}_2\text{WO}_4$ , 0.2 mol/L  $(\text{NH}_4)_2\text{PtCl}_4$  and 0.2 mol/L  $(\text{NH}_4)_2\text{C}_6\text{H}_6\text{O}_7$ , pH = 8.0.

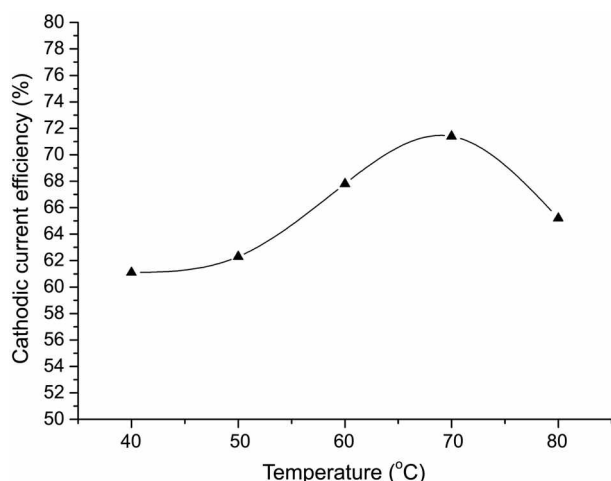


**Figure 4.** Effect of bath temperature on cathodic current efficiency of Co-Pt-W(P) codeposition. Solution composition: 0.1 mol/L CoSO<sub>4</sub>, 0.27 mol/L Na<sub>2</sub>WO<sub>4</sub>, 0.2 mol/L (NH<sub>4</sub>)<sub>2</sub>PtCl<sub>4</sub> and 0.2 mol/L (NH<sub>4</sub>)<sub>2</sub>C<sub>6</sub>H<sub>6</sub>O<sub>7</sub>; pH = 8.0; T = 40 °C-80 °C.

experimental mass). Theoretical mass:  $m_{theo}$  of electrodeposits can be calculated according to Faraday's law. The cathodic current efficiency of Co-Pt-W(P) codeposition is less than 100% as a result of simulation of hydrogen evolution. Figure 4 shows the influence of bath temperature on cathodic current efficiency. It is noticeable that cathodic current efficiency reached the maximum when the bath temperature was 70 °C.

**Influence of temperature on the alloy composition.** Co-Pt-W(P) alloy composition was affected by bath temperature to a large extent. Tungsten and phosphorus content in the Co-Pt-W(P) layers as a function of temperature are shown in Figure 5. Tungsten content in the deposits increases with the bath temperature, while phosphorus content decreases. Experimental results also show that electrolyte temperature affects cobalt and platinum contents faintly. The results shown in Figure 5 indicated that tungsten electrodeposition

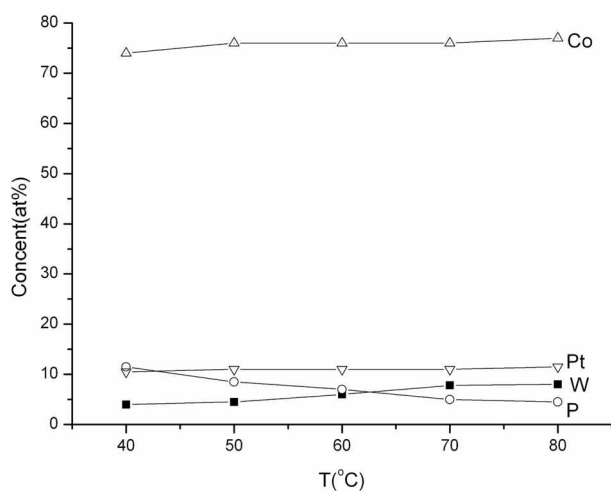


**Figure 5.** Co-Pt-W(P) alloy composition as a function of temperature. Solution composition: 0.1 mol/L CoSO<sub>4</sub>, 0.27 mol/L Na<sub>2</sub>WO<sub>4</sub>, 0.2 mol/L (NH<sub>4</sub>)<sub>2</sub>PtCl<sub>4</sub> and 0.2 mol/L (NH<sub>4</sub>)<sub>2</sub>C<sub>6</sub>H<sub>6</sub>O<sub>7</sub>; pH = 8.0; T = 40 °C-80 °C.

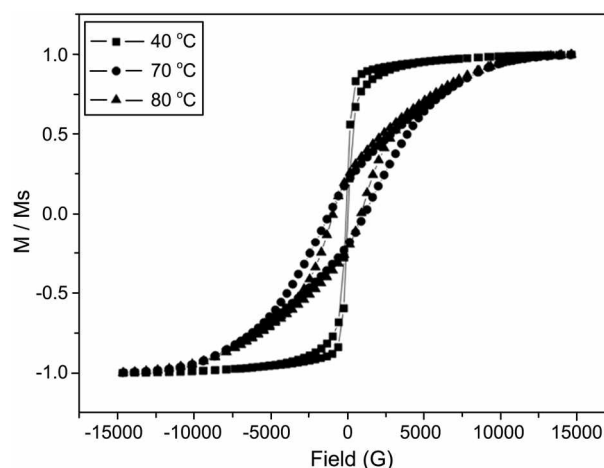


**Figure 6.** Hysteresis loops in the parallel direction at the different temperature. Solution composition: 0.1 mol/L CoSO<sub>4</sub>, 0.27 mol/L Na<sub>2</sub>WO<sub>4</sub>, 0.2 mol/L (NH<sub>4</sub>)<sub>2</sub>PtCl<sub>4</sub> and 0.2 mol/L (NH<sub>4</sub>)<sub>2</sub>C<sub>6</sub>H<sub>6</sub>O<sub>7</sub>; pH = 8.0; T = 40 °C-80 °C.

and phosphorous electrodeposition were restricted by each other, but the detailed mechanism was not clearly understood by far.

**Characterisation of deposits.** The effect of temperature on Co-Pt-W(P) layers' magnetic properties was shown in Figure 6. At low temperature, the films showed soft magnetism. As the electrolyte temperature increased (up to 70 °C), deposits exhibited hard magnetic properties. The increase of tungsten content in the deposit due to temperature increase favors the precipitation of tungsten or tungsten oxide at grain boundaries, which can retard the motion of domain walls.<sup>14</sup> As a result, the coercivity of deposit can be increased. However, with the temperature continued increasing, their hard magnetism would be weakened, because grain size decreased at the higher temperature (see XRD result), a smaller grain size decreased the effective anisotropy of the crystallites and generally results in lower coercivity values.<sup>15,16</sup>

Temperature has an obvious impact on Co-Pt-W(P) alloy

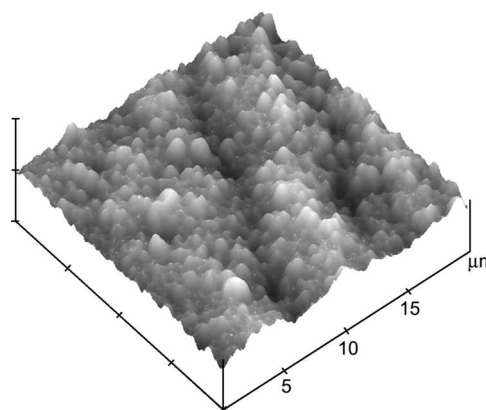


**Figure 7.** Three-dimensional AFM images of Co-Pt-W(P) thin layer (T = 60 °C). Solution composition: 0.1 mol/L CoSO<sub>4</sub>, 0.27 mol/L Na<sub>2</sub>WO<sub>4</sub>, 0.2 mol/L (NH<sub>4</sub>)<sub>2</sub>PtCl<sub>4</sub> and 0.2 mol/L (NH<sub>4</sub>)<sub>2</sub>C<sub>6</sub>H<sub>6</sub>O<sub>7</sub>; pH = 8.0.

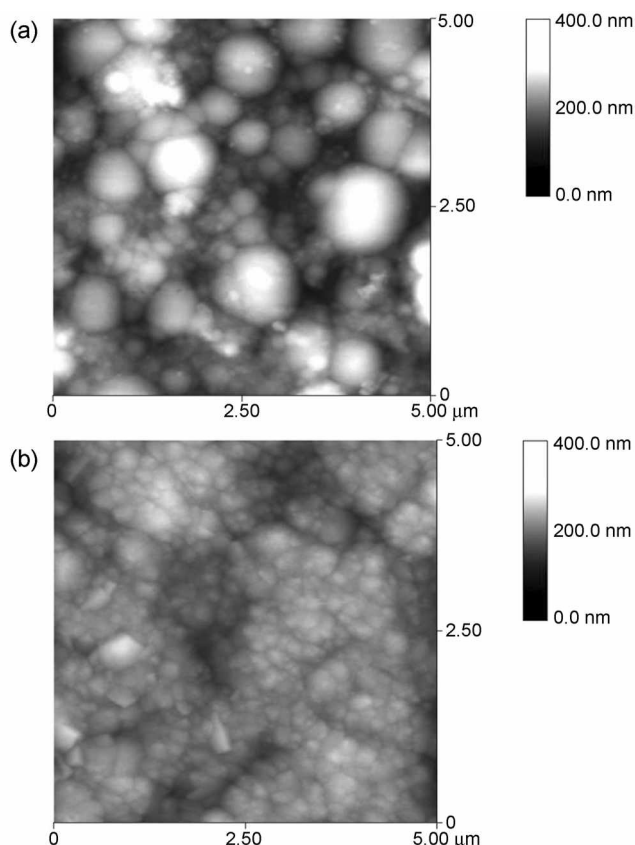


**Figure 8.** AFM images ( $5 \times 5 \mu\text{m}$ ) of Co-Pt-W(P) films electrodeposited at different temperature (a) 40 °C; (b) 80 °C. Solution composition: 0.1 mol/L  $\text{CoSO}_4$ , 0.27 mol/L  $\text{Na}_2\text{WO}_4$ , 0.2 mol/L  $(\text{NH}_4)_2\text{PtCl}_6$  and 0.2 mol/L  $(\text{NH}_4)_2\text{C}_6\text{H}_6\text{O}_7$ ; pH = 8.0.

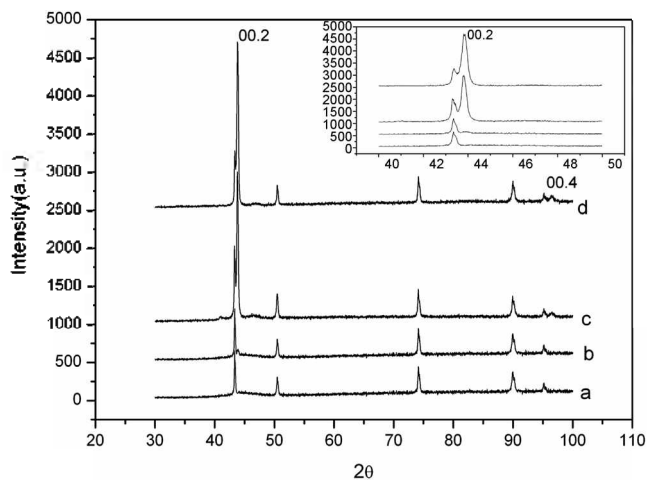


**Figure 9.** XRD pattern of Co-Pt-W alloys. S: copper; temperature (a) 40 °C; (b) 50 °C; (c) 60 °C; (d) 70 °C. Thickness: 0.8  $\mu\text{m}$ . Solution composition: 0.1 mol/L  $\text{CoSO}_4$ , 0.27 mol/L  $\text{Na}_2\text{WO}_4$ , 0.2 mol/L  $(\text{NH}_4)_2\text{PtCl}_6$  and 0.2 mol/L  $(\text{NH}_4)_2\text{C}_6\text{H}_6\text{O}_7$ ; pH = 8.0.

morphology. Figure 7 and Figure 8 show the surface morphology of Co-Pt-W(P) thin films at different bath temperatures. At 60 °C, the crystal grains appeared as isolated growth features and the surface was compact.

The phase structure and texture of Co-Pt-W(P) deposits showed a strong dependence on the electrolyte temperature.

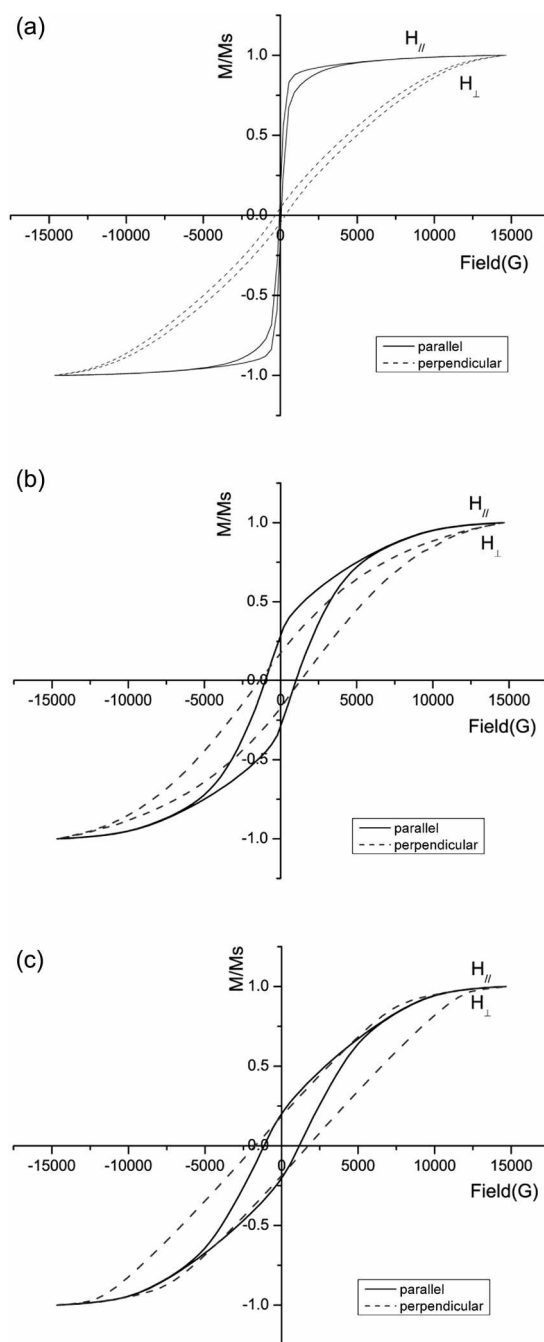


**Figure 10.** Hysteresis loops in the parallel and perpendicular direction at the different temperature. (a) T = 50 °C;  $H_{c||}$ : 61.5 G;  $H_{c\perp}$ : 324.0 G (b) T = 60 °C;  $H_{c||}$ : 1006.8 G;  $H_{c\perp}$ : 1635.0 G (c) T = 70 °C;  $H_{c||}$ : 1150.7 G;  $H_{c\perp}$ : 1945.7 G Thickness: 0.8  $\mu\text{m}$ .

Deposits obtained at 40 °C–70 °C showed hcp structure having basal plane parallel to the surface, *i.e.* [00.1] preferred orientation (P.O.). Moreover, this structure was enhanced by the temperature increase of the solution. According to XRD pattern and Scherrer formula, the grain size of the film was calculated (grain size of deposits at 40 °C was 66.4 nm; grain size of deposits at 80 °C was 44.5 nm).

In Figure 9, with temperature changing from 40 °C to 70 °C, the intensity of [00.1] preferred orientation was strengthened, which led to the improvement of perpendicular

magnetic anisotropy (Figure 10). This is in accordance with the Iulica Zana's theory that magnetocrystalline anisotropy can be regarded as the primary source for the high PMA.<sup>17</sup>

### Summary and Conclusions

When the bath temperature increased, tungsten content in the deposit increased, and phosphorus content decreased. The Co-Pt-W(P) deposits showed a transition from soft to hard magnetic properties as temperature increased. It can be explained by the increase of the precipitation of tungsten or tungsten oxide at grain boundaries. However, higher temperature can weaken hard magnetic properties because of smaller grain size. VSM measurement showed that [00.1] P.O. of Co-Pt-W(P) deposits obtained at 40 °C-70 °C was enhanced by the increase of the temperature. Furthermore, it has been proved that this structure of Co-Pt-W(P) favours perpendicular magnetic anisotropy.

**Acknowledgement.** This work is supported by National Science Foundation of China (No. 20571067& 20601024).

### References

1. Park, D. Y.; Myung, N. V.; Schwartz, M.; Nobe, K. *Electrochim. Acta* **2002**, *47*, 2893.
2. Myunga, N. V.; Park, D. Y.; Yoo, B. Y. *J. Magn. Magn. Mater.* **2003**, *265*, 189.
3. Rhen, F. M. F.; Coey, J. M. D. *J. Magn. Magn. Mater.* **2004**, *272-276*, e883.
4. Feng, W.; Kaori, H.; Sayaka, D.; Okamoto, N. *et al. Electrochem. Commun.* **2004**, *6*, 1149.
5. El-Tabl, A. S. *Bull. Korean Chem. Soc.* **2004**, *25*, 1757.
6. Zana, I.; Zangari, G. *Electrochem. Solid ST* **2003**, *6*, C153.
7. Cavallotti, P. L.; Vicenzo, A.; Bestetti, M.; Franz, S. *Surf. Coat. Tech.* **2003**, *169-170*, 76.
8. Franz, S.; Bestetti, M.; Consonni, M.; Cavallotti, P. L. *Microelectron. Eng.* **2002**, *64*, 487.
9. Qiong, W.; Hongliang, G.; Guoying, W.; Yujian, C. *J. Rare Earths* **2005**, *23*, 46.
10. Cavallotti, P. L.; Bestetti, M.; Franz, S. *Electrochim. Acta* **2003**, *48*, 3013.
11. Qiong, W.; Guoying, W.; Hongliang, G. *J. Funct. Mater.* **2006**, *37*, 1716.
12. Mendoza, L. H.; Robles, J.; Palomar, M. *J. Electroanal. Chem.* **2002**, *521(1)*, 95.
13. Sahari, A.; Azizi, A.; Schmerber, G. *et al. Catal. Today* **2006**, *113(3)*, 257.
14. Franz, S.; Bestetti, M.; Consonni, M. *et al. Microelectron. Eng.* **2002**, *64*, 487.
15. Hoffmann, H.; Fujii, T. *J. Magn. Magn. Mater.* **1993**, *128*, 395.
16. Herzer, G. *IEEE Trans. Magn.* **1990**, *26*, 1397.
17. Zana, I.; Zangari, G.; Shamsuzzoha, M. *J. Magn. Magn. Mater.* **2005**, *292*, 266.